

Design, Synthesis, and Biological Evaluation of Some Heterocyclic Multifunctional Molecular Hybrids for Alzheimer's disease Therapy



Thesis submitted in partial fulfilment for the
Award of Degree

DOCTOR OF PHILOSOPHY

By

Digambar Kumar Waiker

Department of Pharmaceutical Engineering & Technology
Indian Institute of Technology
(Banaras Hindu University)
Varanasi-221005 India

Roll No.17161006

2023



Department of Pharmaceutical Engineering and Technology

CERTIFICATE

It is certified that the work contained in the thesis titled “**Design, Synthesis, and Biological Evaluation of Some Heterocyclic Multifunctional Molecular Hybrids for Alzheimer’s Disease Therapy**” by **Mr. Digambar Kumar Waiker** has been carried out under my supervision and that this work has not been submitted elsewhere for a degree.

It is further certified that the student has fulfilled all the requirements of Comprehensive Examination, Candidacy, and SOTA for the award of Ph.D. Degree.

Date: 19/07/2023

Place: IIT (BHU), Varanasi

23211
19/7/2023

Prof. Sushant Kumar Shrivastava
(Supervisor)

Dr. S. K. SHRIVASTAVA
Professor
Deptt. of Pharm. Engg. and Tech
Indian Institute of Technology
(Banaras Hindu University)
Varanasi-221005

July 17, 2023

CERTIFICATE

It is certified that the work contained in the thesis titled “**Design, Synthesis, and Biological Evaluation of Some Heterocyclic Multifunctional Molecular Hybrids for Alzheimer’s Disease Therapy**” by **Mr. Digambar Kumar Waiker** has been carried out under my co-supervision and that this work has not been submitted elsewhere for a degree.

It is further certified that the student has fulfilled all the requirements of Comprehensive Examination, Candidacy, and SOTA for the award of Ph.D. Degree.



Vincent Jo Davisson, Ph.D. (Co-Supervisor)



Department of Pharmaceutical Engineering and Technology

DECLARATION BY THE CANDIDATE

I, **Digambar Kumar Waiker**, certify that the work embodied in this Ph.D. thesis is my own bonafide work, and was carried out by me under the supervision of **Prof. Sushant Kumar Shrivastava** from **July 2017 to June 2023** at the **Department of Pharmaceutical Engineering & Technology, Indian Institute of Technology (Banaras Hindu University), Varanasi**. The matter embodied in this Ph.D. thesis has not been submitted for the award of any other degree/diploma.

I declare that I have faithfully acknowledged and given credit to the research workers wherever their works have been cited in my work in this thesis. I further declare that I have not willfully copied any other's work, paragraphs, text, data, results, etc. reported in the journals, books, magazines, reports, dissertations, theses, *etc.*, or available at websites and have not included them in this Ph.D. thesis and have not cited as my own work.

Date: 19/07/2023



19/07/2023

Place: IIT (BHU), Varanasi

Digambar Kumar Waiker

It is certified that the above statement made by the student is correct to the best of our knowledge.

CERTIFICATE BY THE SUPERVISOR AND HEAD OF THE DEPARTMENT


19/7/2023
Prof. Sushant Kumar Shrivastava
(Supervisor)

Dr. S. K. SHRIVASTAVA
Professor
Deptt. of Pharm. Engg. and Tech
Indian Institute of Technology
(Banaras Hindu University)
Varanasi-221005


19/7/23
(Head of the Department)
विभागाध्यक्ष / Head

मैद्युकीय अभियांत्रिकी एवं प्रौद्योगिकी विभाग /
Department of Pharmaceutical Engineering & Technology
भारतीय प्रौद्योगिकी संस्थान / INDIAN INSTITUTE OF TECHNOLOGY
(बनारस हिन्दू विश्वविद्यालय) / (BANARAS HINDU UNIVERSITY)
वाराणसी-221005 / Varanasi-221005



Department of Pharmaceutical Engineering and Technology

COPYRIGHT TRANSFER CERTIFICATE

Title of the Thesis : Design, Synthesis, and Biological Evaluation of Small
Molecular Hybrids as Multitarget Directed Ligands for
Alzheimer's disease Therapy

Candidate's Name : Mr. Digambar Kumar Waiker

Copyright Transfer

The undersigned hereby assigns to the Indian Institute of Technology (Banaras Hindu University), Varanasi all rights under copyright that may exist in and for the above thesis submitted for the award of the Ph.D. degree.

Date: 19/07/2023

Place: IIT (BHU), Varanasi

Digambar Kumar Waiker

Note: However, the author may reproduce or authorize others to reproduce material extracted verbatim from the thesis or derivative of the thesis for the author's personal use provided that the source and University's copyright notice are indicated.

Acknowledgments

I bow to the feet of **Bharat Ratna Pandit Madan Mohan Malaviyaji**, founder of the Banaras Hindu University which is his crowning achievement. Living in his abode, I always felt a sense of holiness. It is a stupendous monument to his peculiar genius, his audacity in conception, and his persistence in execution. The University symbolizes Malviyaji's respect for the past, confidence in the present, and hope for the future generation of India.

It is a matter of privilege and joy to express my feelings of gratitude to **Prof. Sushant Kumar Shrivastava**. I am thankful for his continuous support throughout my research for his patience, motivation, and immense knowledge. I am indebted to him for his appreciation for success and backing and support in failures, which ultimately made me keen to tackle any obstructions occurring during the research work. Without his supervision and constant help, this dissertation would not have been possible. He also helped me a lot as Head, of the Department of Pharmaceutical Engineering & Technology, Indian Institute of Technology (Banaras Hindu University), Varanasi to use the department facilities to carry out my research work.

I would also like to convey my heartfelt thanks to **Prof. Vincent Jo Davisson**, who invited me to **the** Department of Medicinal Chemistry and Molecular Pharmacology, Purdue University, IN, USA under the SERB-OVDF scheme as a visiting scholar and provided me with his research lab facilities. I also thank him for his continuous motivation, and support and also for giving me his consent to become co-supervisor of my Ph.D. research work. I would also like to thank him for providing financial support in performing the kinase screening assay.

I am also thankful to **Prof. Piyush Trivedi**, Ex Vice-chancellor, Rajiv Gandhi Pradyogiki Vishwavidyalaya Bhopal for his continuous support, motivation, and constant help throughout my research.

I am also grateful to, **Prof. B. Mishra, Prof. S.K. Singh & Prof. Sanjay Singh**, Former Heads, for their constant inspiration, valuable suggestions, and help which have led to the successful completion of this work.

I owe my gratitude to all my respected Research Progress and Evaluation Committee (RPEC) members for their encouragement and insightful comments leading me to the completion of the research work.

I would like to thank *Prof. Sairam Krishnamurthy* and *Dr. Vinod Tiwari* for their continuous support in performing *in vivo/ex vivo* experiments.

I would also like to thank *Dr. Senthil Raja A., Dr. Gyan P. Modi, Dr. Shreyans K. Jain,* and all other faculty members of the Department for their support and encouragement.

I also express my sincere thanks to *Prof. Surendra Kumar Trigun, Prof. S. Saikrishna, and Prof. S.P. Sing,* Faculty of Science, Banaras Hindu University, Varanasi for their help in performing *ex vivo* studies.

I also acknowledge the **Council of Scientific and Industrial Research-Human Resource Development Group (CSIR-HRDG)** and **Science & Engineering Research Board (SERB- Govt. of India** for providing me senior research fellowship (CSIR SRF-direct) and overseas visiting doctoral fellowship (SERB-Purdue, OVDF) to carry out my Ph.D. research in India and Purdue University, IN, U.S.A. respectively.

I am also grateful to ***all the non-teaching staff*** of the Department for their timely assistance and co-operation during the period of my Ph.D. research.

I am indeed thankful to have the company of my seniors *Mr. Piyoosh Sharma, Mr. Ankit Seth, Mr. Prabhash Nath Tripathi, Mr. Avanish Tripathi;* my colleagues *Ms. Swetha Rayala, Mr. Tarkeshwar Dubey, Ms. Sangita Hazarika, Ms. Pratigya Tripathi, Ms. Prabha Rajput, Ms. Varsha Rani, Mr. Subhjit Makar;* my juniors *Mr. Akash Verma, Ms. Poorvi Saraf, Ms. Bhagwati Bhardwaj, Mr. Hansal Kumar, Mr. Abhinav Singh, Mr. Pidugu Venkata Ravi Kiran, Ms. Deeksha and Mr. Kshirod* and juniors who were ever ready to provide me with all the possible help.

A special thanks to my family. Words cannot express how grateful I am to all my ***family members*** for all of the sacrifices that they made on my behalf and the continuous support they provided to me. Most importantly, none of this would have been possible without the love and patience of my ***parents, wife, daughter, younger brother, and other family members.*** They have been a constant source of love, moral support, and strength all these years. I owe this achievement to them.

Last but not least, I pray for the ***animals*** who sacrificed themselves for the cause of my research work.

Date: 19/07/2023

Place: IIT (BHU) Varanasi



Digambar Kumar Waiker

INDEX

Contents	Page No.
List of Figures	xii
List of Tables	xxii
Abbreviations and Symbols	xxiii
Preface	xxvii
CHAPTER 1. INTRODUCTION	1
1.1 Alzheimer's disease	1
1.2 Pathophysiology involved in AD	2
1.2.1 Cholinergic hypothesis	3
1.2.2 Amyloid beta (A β) hypothesis	5
1.2.3 Tau hypothesis	6
1.2.4 Excitotoxic hypothesis	8
1.2.5 Oxidative stress hypothesis	8
1.2.6 Mitochondrial hypothesis	9
1.2.7 Neuroinflammation	10
1.2.8 Dyrk1A hypothesis	11
1.2.9 Apolipoprotein E (APO ϵ 4) hypothesis	12
1.3 Available treatment for AD	12
1.4 Newer therapeutic approaches to develop compounds for the treatment of AD	12
1.4.1 Multitarget approach	14
1.4.2 Computer-aided drug design approach	15
1.4.3 Molecular hybridization	16
1.5 Design hypothesis in the present study	16
CHAPTER 2. REVIEW OF LITERATURE	19
2.1. 1,3,4-Oxadiazoles as multitarget directed ligands in AD	19
2.2. Piperazines and Benzylpiperidine as MTDL	27
CHAPTER 3. RATIONALE, OBJECTIVES AND PLAN OF WORK	45
3.1. Rationale and objectives	45
3.1.1 Designing of part I (Series I) Molecular hybrids	46
3.1.2 Designing of part II (Series II & III) Molecular hybrids	47
3.2. Plan of work	50
3.3 Significance of the study	51
CHAPTER 4. EXPERIMENTAL	52
4.1 Computational studies	52
4.1.1 Pharmacophore modeling	52

Contents	Page No.
4.1.2 Virtual screening and docking-post processing (DPP)	52
4.1.3 Mechanics-Generalized Born Surface Area (MM-GBSA)	53
4.1.4 Molecular docking study	53
4.1.5 Molecular dynamics and simulations study	54
4.1.6 In silico drug likeness determination	54
4.1.7 DFT and Fukui function calculations	55
4.2 Synthesis	55
4.2.1 Chemicals and reagents	55
4.2.1.1 Series-I : 3-NH linked benzylpiperazine derivatives of 5-phenyl-1,3,4-oxadiazole 2-thione (SD 1-17)	55
4.2.1.2 General procedure A for the synthesis of compound (B1-17, 2 and 2a-q).	56
4.2.1.3 General procedure B for the synthesis of compound (C1-17, 3 and 3a-q).	56
4.2.1.4 General procedure for the synthesis of compound (SD 1-17)	57
4.2.2 Series-II : 3-NH linked substituted piperazine derivatives of 5-phenyl-1,3,4-oxadiazole 2-thione (4 a-j)	57
4.2.2.1 General procedure for synthesis of compounds (4a-j)	58
4.2.3 Series-III : 2-thiol linked N-(1-benzylpiperidin-4-yl)-2-chloroacetamide derivatives of 5-phenyl-1,3,4-oxadiazole 2-thione 1,3,4-oxadiazoles tethered with an —NH linker (5a-q)	58
4.2.3.1 General procedure for synthesis of compound NPBC	58
4.2.3.2 General procedure for synthesis of compounds (5a-q)	59
4.3 Characterization of the synthesized compounds	59
4.3.1 Melting point	59
4.3.2 TLC (R_f value)	59
4.3.3 FT-IR	60
4.3.4 ^1H NMR and ^{13}C NMR	60
4.3.5 Mass spectra	60
4.3.6 Single crystal X-Ray Crystallography	60
4.3.7 Determination of percentage purity by HPLC	61
4.4 Biological Evaluation	61
4.4.1 Pharmacology (<i>In vitro</i> studies)	61
4.4.1.1 Human Cholinesterase (hAChE and hBChE) inhibition assay to determine IC_{50} values	61
4.4.1.2 Enzyme kinetics study	62
4.4.1.3 BACE-1 inhibition study	62
4.4.1.4 Propidium iodide displacement assay	63

Contents	Page No.
4.4.1.5 Parallel artificial membrane permeation (PAMPA) assay	63
4.4.1.6 Neuroprotective studies on SH-SY5Y cell lines	64
4.4.1.6.1 Differentiation of SH-SY5Y cell lines	64
4.4.1.6.2 MTT assay	64
4.4.1.6.3 Effect of drug and standard on the morphology of differentiated SH-SY5Y cells	65
4.4.1.7 Anti-A β aggregation activity	65
4.4.1.7.1 Thioflavin T assay	65
4.4.1.7.2 Confocal microscopy	66
4.4.1.7.3 AFM study	66
4.4.1.7.4 SEM analysis	67
4.4.2 <i>In vivo</i> behavioral and <i>ex vivo</i> studies	67
4.4.2.1 Animals	67
4.4.2.2 Acute oral toxicity study	67
4.4.2.3 Scopolamine-induced amnesia models for testing cognition enhancement in rat/mice	68
4.4.2.4 <i>Ex Vivo and biochemical analysis in scopolamine-induced model</i>	69
4.4.2.5 qRT-PCR analysis of proinflammatory cytokines (TNF- α and IL- β) in scopolamine-induced model	71
4.4.2.6 A β -induced Morris water maze test	72
4.4.2.7 Western-blot analysis	73
4.4.2.8 Immunohistochemistry	73
4.4.2.9 Brain tissue histopathology	74
CHAPTER 5. RESULTS AND DISCUSSION	75
5.1 PART-I: SERIES I	75
5.1.1 Chemistry	75
5.1.1.1 Synthesis of Series I (SD 1-17): Substituted 1,3,4-oxadiazole-2-thione linked benzylpiperazine derivatives	75
5.1.1.2 Characterization of the synthesized compounds (Series I, SD 1-17)	76
5.1.2 Biological evaluation	83
5.1.2.1 Pharmacology (<i>In vitro</i> studies)	83
5.1.2.2 <i>In vivo</i> and <i>ex vivo</i> studies	94
5.1.3 In silico studies	101
5.2 PART-II: SERIES II–V	111
5.2.1 Computational studies	111
5.2.1.1 Pharmacophore modelling	111
5.2.1.2 Virtual screening	112
5.2.1.3 Molecular docking	112
5.2.1.4 MMGB-SA	116

Contents	Page No.
5.2.1.5 Molecular dynamics simulation	117
5.2.1.6 Density Function calculation	123
5.2.1.7 In-silico prediction of Drug likeness	125
5.2.2 Chemistry	126
5.2.2.1 Synthesis of Series II (4a-j) and III (5a-q) compounds: 1.3.4-oxadiazole-2-thiol linked with substituted piperazines and N-(1-benzylpiperidin-4-yl)-2- chloroacetamide (NBPC)	126
5.2.2.2 Characterization of the synthesized compounds (Series II and III)	128
5.2.3 Biological evaluation	143
5.2.3.1 <i>In vitro</i> studies	143
5.2.3.2 <i>In vivo</i> and <i>ex vivo</i> studies	157
CHAPTER 6. SUMMARY AND CONCLUSION	171
6.1. Summary and Conclusion	171
6.2 Scope and future directions	174
CHAPTER 7. REFERENCES	176
CHAPTER 8. APPENDIX	199
8.1. ¹ H and ¹³ C spectra of representative synthesized compounds	199
8.2. Mass spectra of representative synthesized compounds	223
8.3 HPLC chromatograms of representative synthesized compounds	230
LIST OF PUBLICATIONS	233

LIST OF FIGURES

Fig. No.	Figure Legends	Page No.
1.1	Release of ACh and normal neurotransmission process.	4
1.2	Amyloidogenic (β -secretase assisted) and non-amyloidogenic (α -secretase assisted) pathways of A β formation.	6
1.3	Formation of neurofibrillary tangles (NFTs), and neuronal dysfunction associated to tau phosphorylation.	7
1.4	Multitargeting inhibitory approaches for the treatment of Alzheimer's disease.	17
2.1	1,3,4-Oxadiazole compound as GSK-3 β , CDK-5 inhibitor (1), ChE and LOX inhibitors (2-5).	19
2.2	1,3,4-Oxadiazole scaffold containing analogous (5-8)	20
2.3	Novel benzothiazole tethered 1,3,4-oxadiazole hybrids (9-12).	21
2.4	3-Piperidinyl-1,3,4-oxadiazole molecular hybrid (13) with AChE inhibitory potential.	21
2.5	A multifunctional molecular hybrid of 1,3,4-oxadiazoles (14-17) to treat AD.	22
2.6	A N-benzylpyrrolidine linked 1,3,4-oxadiazoles (18-21) MTDL to treat AD.	24
2.7	A multifunctional molecular hybrid of 1,3,4-oxadiazoles (22-23) for AD therapy.	25
2.8	A dual-targeting molecular hybrids of 1,3,4-oxadiazoles (24) to treat AD.	25
2.9	1,3,4-oxadiazoles/thiazole molecular hybrids (25-28) as dual ChE inhibitors against AD.	26
2.10	Potential MTDL of 1,3,4-oxadiazoles (25-28) for the treatment of AD.	27
2.11	The piperazine-tethered cyclopentathiophene (34-35) and benzylpiperidine substituted analogs (36) as multifunctional agents against AD.	28
2.12	Molecular hybrids of N-benzylpiperidine and 2-aminopyridine-3,5 dicarbonitrile as multifunctional hybrids (37-38).	29
2.13	Piperazine linked molecular hybrids (39-42) as MTDLs for AD treatment.	30
2.14	Phthalimide (43) and Coumarin (44-47) link piperazine and N-benzylpiperidine derivatives as multifunctional molecular hybrids.	31
2.15	Molecular hybrids of N-benzylpiperidine (48-49) and piperazine derivatives (50-51) as multifunctional agents for AD therapy.	31
2.16	The N-benzylpiperidine and indole molecular hybrid (52) with multitargeted activities against AD.	32

Fig. No.	Figure Legends	Page No.
2.17	Ferulic acid-based <i>N</i> -benzylpiperidine hybrids (53-57) as MTDLs.	33
2.18	<i>N</i> -benzylpiperidine linked diarylthiazole (58) and coumarin compound (59) as potential multitargeted ligand against AD.	34
2.19	Umbelic (60) and caffeic acid-based molecular hybrids (61) of <i>N</i> -benzylpiperidine.	35
2.20	Molecular hybrids of <i>N</i> -benzylpiperidine (62-63) as MTDLs.	36
2.21	Benzthiazole linked piperazine compounds (64-65) as MTDLs.	36
2.22	Piperazine derivatives (66-68) as multifunctional agents for AD treatment.	37
2.23	Piperazine linked benzimidazole compounds (69-70) and L- and D-glutamic acid linked benzylpiperidine compound (71) as MTDL for AD therapy.	38
2.24	Donepezil like molecular hybrids of <i>N</i> -benzylpiperidine linked benzimidazole (72) and benzofuran (73) compounds and 2-aminopyridine-3,5-dicarbonitrile.	39
2.25	Tacrine (74) and isoxazole (75) linked benzylpiperazine derivatives and as multifunctional agents for AD treatment.	39
2.26	Benzylpiperazine linked deoxyvasicinone derivatives as multifunctional agents (76-79) for AD treatment.	40
2.27	Molecular hybrids of 1H-pyrazolo[3,4-b]pyridine as MTDL for AD therapy (80-82).	40
2.28	Novel <i>N</i> -benzylpiperidine carboxamide derivatives (83-84) and benzylamine linked multifunctional hybrids (85-86)	41
2.29	Molecular hybrids of <i>N</i> -benzylpiperidine tethered benzimidazole (87-89) and amidine (90) and benzthiazole (91) linked piperazine analogs as MTDL for AD treatment.	42
2.30	Molecular hybrids of <i>N</i> -benzylpiperidine (92-93) and piperin linked piperazine compounds as dual ChE inhibitors.	43
3.1	Designing strategy of the present series of compounds SD1-17 using molecular hybridization approach.	47
3.2	Identified hits and design strategy for the present series of compounds (4a-j and 5a-q)	49
5.1	Enzyme kinetics results of compound SD-6 against hAChE; A) Lineweaver-Burk Plot showing mixed type non-competitive inhibition; B) Dixon plot showing K_i on intersecting point of the negative x -axis.	86

Fig. No.	Figure Legends	Page No.
5.2	SAR of the compounds SD1-17	88
5.3	Neurotoxicity and neuroprotective estimation of compounds SD-4 and SD-6 ; A) Cytotoxicity estimation of compounds SD-4 and SD-6 along with donepezil on differentiated SH-SY5Y cell lines B) Neuroprotective estimation of SD-4 , SD-6 , and donepezil on non-differentiated SH-SY5Y cell lines in presence of H ₂ O ₂ (200 μM). (^a p < 0.01) compared to the control. (^{a,b} p < 0.05) (^{a,b,c} p < 0.01) (^{b,c,d} p < 0.001) compared to H ₂ O ₂ treated.	91
5.4	Morphological estimation of neurotoxicity profile of the compounds SD-4 and SD-6 in RA/BDNF differentiated SH-SY5Y cells A) Differentiated SH-SY5Y cells alone; B) Cell morphology after incubation with compound SD-4 (40 μM) for 24 h; C) Cell morphology after incubation with compound SD-6 (40 μM) for 24 h; cell morphology after incubation with donepezil (40 μM) for 24 h. The images were captured through phase contrast microscopy.	91
5.5	Cell morphology estimation of neuroprotective activity of compounds SD-4 and SD-6 on non-differentiated SH-SY5Y cells upon co-treatment with H ₂ O ₂ A) Cells without treatment; B) cells upon H ₂ O ₂ treatment only; C) Cells treated with SD-4 (20 μM) in the presence of H ₂ O ₂ (200 μM); D) Cells treated with SD-6 (20 μM) in the presence of H ₂ O ₂ (200 μM). The images were captured through Phase contrast microscopy.	92
5.6	Anti-Aβ aggregation experiments of compounds SD-4 and SD-6 : A) Self-induced % anti-Aβ aggregation: B) AChE-induced % anti-Aβ aggregation: C) Self-induced anti-Aβ aggregation reduced NFI: D) AChE-induced anti-Aβ aggregation reduced NFI.	93
5.7	Histopathology of the animal organs after acute toxicity investigation through H & E staining; A) Kidney tissue showing normal DCT, PCT, and Glomerulus; B) Liver tissue showing the presence of normal Kuepfer cells; C) Normal lung tissue; D) Heart image showing normal cardiac muscles.	95
5.8	Estimation of SD-6 and donepezil effects in cognition and memory improvement in scopolamine-induced behavioral models by Y-maze test; A) % spontaneous alterations; B) a total number of arm entries, All results are expressed in mean ± SEM (n=6). (^a p < 0.001) vs control. (^{a,b} p < 0.05), (^{a,b,c} p < 0.01) and (^{b,c,d} p < 0.001) vs scopolamine, (^b p < 0.001) vs scopolamine.	96

Fig. No.	Figure Legends	Page No.
5.9	Estimation of SD-6 and donepezil effects in ICV $A\beta_{1-42}$ induced Morris water maze test; A) escape latency; B) Time spent in the platform quadrant in the probe trial; C) a number of entries to the platform zone during probe trial, All results are expressed in mean \pm SEM (n=6). (^a p < 0.001 vs. control, and ^b p < 0.001 vs. an $A\beta$).	98
5.10	<i>Ex vivo</i> studies of the compound SD-6 to estimate the levels of A) AChE: B) Acetylcholine (ACh): C) MDA: D) SOD: E) GSH: and F) Catalase. The results are expressed as mean \pm SEM (n=6), (^a p < 0.001) vs control. (^{a,b} p < 0.05), (^{a,b,c} p < 0.01) and (^{b,c,d} p < 0.001) vs scopolamine.	100
5.11	Histomorphological representation dentate gyrus (DG) region of brain hippocampal of the control (A); $A\beta_{1-42}$ treated group (B); SD-6 treated (10 mg/kg) group (C); donepezil (DNZ) treated (5mg/kg) group (D); and density graph of total neuronal cells (% of control) present in DG (E).	101
5.12	Molecular docking 3D interaction representation of the compounds SD-4 and SD-6 with hAChE (PDB: 4EV7) and hBACE-1 (PDB: 2ZJM): A) 3D docked pose of compound SD-4 with hAChE; B) 3D docked pose of compound SD-6 with hAChE; C) 3D docked pose of compound SD-4 with hBACE-1; D) 3D docked pose of compound SD-6 with hBACE-1; E) 3D docked superimposition of compound SD-4 , SD-6 (bold gray sticks) and donepezil (green sticks) with hAChE; F) 3D docked superimposition of compound SD-4 , SD-6 (gray and bold yellow sticks) and F1M (bold blue sticks) with hBACE-1.	102
5.13	Results of 100 ns MD simulation run of the compound SD-4 complexed with hAChE (PDB: 4EY7); A) 2D interaction diagram representing the interaction of the molecule with amino acid residues; B) ligand-protein interaction histogram showing interaction fractions (e.g. for a value of 0.6 indicates 60% of interaction in total simulation run); C) ligand-protein RMSD relative to protein backbone structure; D) time-line graphical representation showing interaction with individual residues in each trajectory frame.	106
5.14	Results of 100 ns MD simulation run of the compound SD-4 complexed with hBChE (PDB: 4TPK); A) 2D interaction diagram representing the interaction of the molecule with amino acid residues; B) ligand-protein interaction histogram showing interaction fraction (e.g. for a value of 0.8 indicates 80% of interaction	107

Fig. No.	Figure Legends	Page No.
	in total simulation run); C) ligand-protein RMSD relative to protein backbone structure; D) time-line graphical representation showing interaction with individual residues in each trajectory frame.	
5.15	Results of 100 ns MD simulation run of the compound SD-4 complexed with hBACE-1 (PDB: 2ZJM); A) 2D interaction diagram representing the interaction of the molecule with amino acid residues; B) ligand-protein interaction histogram showing interaction fractions (e.g. for a value of 0.6 indicates 60% of interaction in total simulation run); C) ligand-protein RMSD relative to protein backbone structure; D) time-line graphical representation showing interaction with individual residues in each trajectory frame.	107
5.16	Results of 100 ns MD simulation run of the compound SD-6 complexed with hAChE (PDB: 4EY7); A) 2D interaction diagram representing the interaction of the molecule with amino acid residues; B) ligand-protein interaction histogram showing interaction fractions (e.g. for a value of 0.6 indicates 60% of interaction in total simulation run); C) ligand-protein RMSD relative to protein backbone structure; D) time-line graphical representation showing interaction with individual residues in each trajectory frame.	108
5.17	Results of 100 ns MD simulation run of the compound SD-4 complexed with hBChE (PDB: 4TPK); A) 2D interaction diagram representing the interaction of the molecule with amino acid residues; B) ligand-protein interaction histogram showing interaction fraction (e.g. for a value of 0.8 indicates 80% of interaction in total simulation run); C) ligand-protein RMSD relative to protein backbone structure; D) time-line graphical representation showing interaction with individual residues in each trajectory frame.	108
5.18	Results of 100 ns MD simulation run of the compound SD-6 complexed with hBChE (PDB: 4TPK); A) 2D interaction diagram representing the interaction of the molecule with amino acid residues; B) ligand-protein interaction histogram showing interaction fraction (e.g. for a value of 0.8 indicates 80% of interaction in total simulation run); C) ligand-protein RMSD relative to protein backbone structure; D) time-line graphical representation showing interaction with individual residues in each trajectory frame.	109
5.19	e-Pharmacophore models A) AChE (PDB: 4EY7) B) BACE-1 (PDB: 2ZJM)	112

Fig. No.	Figure Legends	Page No.
5.20	Molecular Docking studies of the compound 5d in the active site of the enzymes. A & B) 2D and 3D representation of compound 5d in hAChE active site (PDB: 4EY7); C & D) 2D and 3D representation of compound 5d in hBChE active site (PDB: 4TPK) E & F) 2D and 3D representation of compound 5d in hBACE-1 active site (PDB: 2ZJM).	114
5.21	Molecular Docking studies of the compound 5f in the active site of the enzymes. A & B) 2D and 3D representation of compound 5f in hAChE active site (PDB: 4EY7); C & D) 2D and 3D representation of compound 5f in hBChE active site (PDB: 4TPK) E & F) 2D and 3D representation of compound 5f in hBACE-1 active site (PDB: 2ZJM).	115
5.22	Molecular dynamics (MD) studies of compound 5d -AChE (4EY7) docked complex. (A) 2D representation showing % interaction with amino acid residues in the active site; B) Histogram presentation of interaction fraction with amino acid residues; C) RMSD graph of ligand-protein (5d -AChE) interaction of 100 ns MD; D) Timeline graph indicating all amino acid interactions with the ligand on each time frame.	119
5.23	Molecular dynamics (MD) studies of compound 5f -hAChE (4EY7) docked complex. (A) 2D representation showing % interaction with amino acid residues in the active site; B) Histogram presentation of interaction fraction with amino acid residues; C) RMSD graph of ligand-protein (5f -AChE) interaction of 100 ns MD; D) Timeline graph indicating all amino acid interactions with the ligand on each time frame.	120
5.24	Molecular dynamics (MD) studies of compound 5d -BChE (4TPK) docked complex. (A) 2D representation showing % interaction with amino acid residues in the active site; B) Histogram presentation of interaction fraction with amino acid residues; C) RMSD graph of ligand-protein (5d -BChE) interaction of 100 ns MD; D) Timeline graph indicating all amino acid.	120
5.25	Molecular dynamics (MD) studies of compound 5f -BChE (4TPK) docked complex. (A) 2D representation showing % interaction with amino acid residues in the active site; B) Histogram presentation of interaction fraction with amino acid residues; C) RMSD graph of ligand-protein (5f -BChE) interaction of 100 ns MD;	121

Fig. No.	Figure Legends	Page No.
	D) Timeline graph indicating all amino acid interactions with the ligand on each time frame.	121
5.26	Molecular dynamics (MD) studies of compound 5d -BACE-1 (2ZJ7) docked complex. (A) 2D representation showing % interaction with amino acid residues in the active site; B) Histogram presentation of interaction fraction with amino acid residues; C) RMSD graph of ligand-protein (5d -BACE-1) interaction of 100 ns MD; D) Timeline graph indicating all amino acid interactions with the ligand on each time frame.	122
5.27	Molecular dynamics (MD) studies of compound 5f -BACE-1 (2ZJ7) docked complex. (A) 2D representation showing % interaction with amino acid residues in the active site; B) Histogram presentation of interaction fraction with amino acid residues; C) RMSD graph of ligand-protein (5f -BACE-1) interaction of 100 ns MD; D) Timeline graph indicating all amino acid interactions with the ligand on each time frame.	122
5.28	Molecular dynamics (MD) studies of 100 ns for the compound 5d and 5f against AChE and BACE-1 enzyme complex showing active site molecular interactions; (A) 5d -AChE complex B) 5d -BACE-1 complex; C) 5f -AChE complex; D) 5f -BACE-1 complex.	123
5.29	HOMO-LUMO orbital density and molecular electrostatic potential (MEP) surface of the compound 5d and 5f ; A & C) HOMO and LUMO orbital density of compound 5d , B & D) HOMO and LUMO orbital density of compound 5f ; E & F) molecular electrostatic potential (MEP) surface of the compound 5d and 5f .	124
5.30	Graphical representation of electrophilic fukui function + ve $f(r)$ left column and nucleophilic fukui function- ve $f(r)$ right column of the compounds 5d and 5f .	142
5.31	ORTEP diagram of compound 5f obtained at 100 K	147
5.32	The enzyme kinetics study of 5d and 5f compounds determined using Lineweaver-Burk double reciprocal plots, showing inhibition patterns A) hAChE inhibition by compound 5d using ATCI as substrate; B) hAChE inhibition by compound 5f using ATCI as substrate; C) Dixon plot showing dissociation constant K_i of the compound 5d : D) Dixon plot showing dissociation constant K_i of the compound 5f .	149

Fig. No.	Figure Legends	Page No.
5.33	Structure activity relationship of the compounds 4a-j and 5a-q	156
5.34	Analysis of % cell viability and cell morphology on differentiated SH-SY5Y neuroblastoma cell lines after treatment with compounds; A) SH-SY5Y cell lines incubated with 10, 20 40, and 80 μ M concentration of donepezil, 5d , and 5f ; B) % cell viability of non-differentiated and differentiated SH-SY5Y cells incubated with $A\beta_{1-42}$ alone and 5d and 5f for 72 h; C) Differentiated SH-SY5Y cell lines: D) Differentiated SH-SY5Y cell lines treated with standard donepezil; E) Differentiated SH-SY5Y cell lines treated with compound 5d ; F) Differentiated SH-SY5Y cell lines treated with compound 5f .	152
5.35	Results of % cell viability assay A) SH-SY5Y cell lines incubated with 10, 20 40, and 80 μ M concentrations of donepezil, 5d , and 5f ; B) % cell viability of non-differentiated and differentiated SH-SY5Y cells incubated with $A\beta_{1-42}$ alone and 5d and 5f for 72 h; C) SH-SY5Y cells treated with $A\beta_{1-42}$; D) incubation of $A\beta_{1-42}$ treated SH-SY5Y cells with compound 5d ; E) incubation of $A\beta_{1-42}$ treated SH-SY5Y cells with 5f . Data are displayed as mean \pm SD of three independent experiments (n=3).	153
5.36	Anti- $A\beta$ aggregation effect of compound 5d and 5f compared with standard donepezil: A) self-induced % anti- $A\beta$ aggregation experiment; B) hAChE-induced anti- $A\beta$ aggregation experiment. Data are expressed as mean \pm SEM of three independent experiments (n=3).	155
5.37	Thioflavin T assay of compounds 5d and 5f ; A) Self- induced $A\beta$ aggregation B) hAChE-induced $A\beta$ aggregation: C) Confocal microscopy images blank (PBS), $A\beta$ (monomers) 0 h, and $A\beta$ after 48 h (aggregates) ; D) confocal images of anti- $A\beta$ aggregation effects of compounds 5d , 5f and standard curcumin after 24 and 48 h in presence of (ThT).	155
5.38	AFM and SEM analysis of $A\beta$ aggregation inhibition by compounds 5d , 5f , and curcumin at different time points: A) 2D representation of AFM studies showing anti $A\beta$ aggregation at 10 μ M concentration on day 1, 3, and 5; B) 3D representation of AFM studies showing anti $A\beta$ aggregation at 10 μ M concentration on day 1, 3, and 5; C) 2D representation of SEM studies showing anti $A\beta$ aggregation at 10 μ M concentration on day 1, 3, and 5.	157
5.39	Histopathological examination of the different animal organs via H & E staining after acute toxicity studies; A) brain tissue showing normal hippocampus and	158

Fig. No.	Figure Legends	Page No.
	cortex; B) Liver tissue showing the presence of normal Kuepfer cells; C) Kidney tissue showing normal DCT, PCT, and Glomerulus; D) Heart slice showing normal cardiac muscles.	
5.40	Elevated plus maze test of compound 5d and 5f A) retention transfer latency of compound 5d ; B) % ITL of compound 5d ; C) Total time latency of compound 5d ; D) retention transfer latency of compound 5f ; E) % ITL of compound 5f ; F) Total time latency of compound. Data represented as mean \pm SEM (n=6). ***p < 0.001, **p < 0.01, *p < 0.05 vs scopolamine; #### p < 0.001vs Naïve.	160
5.41	<i>Ex vivo</i> estimation of effects of compound 5d in scopolamine-induced mice brain hippocampus and cortex; A) & B) AChE activity estimation; C) & D) Thiobarbituric acid reactive substance (TBARS) assay to estimate MDA levels; E) & F) Glutathione (GSH) estimation to evaluate ROS generation against induced oxidative stress; G) & H) estimation of nitrite (NO) levels. Data represented as mean \pm SEM (n=6). ***p < 0.001, **p < 0.01, *p < 0.05 vs scopolamine; #### p < 0.001vs Naïve, NS = non-significant.	162
5.42	<i>Ex vivo</i> estimation of effects of compound 5f in scopolamine-induced mice brain hippocampus and cortex; A) & B) AChE activity estimation; C) & D) Thiobarbituric acid reactive substance (TBARS) assay to estimate MDA levels; E) & F) Glutathione (GSH) estimation to evaluate ROS generation against induced oxidative stress; G) & H) estimation of nitrite (NO) levels. Data represented as mean \pm SEM (n=6). ***p < 0.001, **p < 0.01, *p < 0.05 vs scopolamine; #### p < 0.001vs Naïve, ns = non-significant.	163
5.43	qRT-PCR analysis of neuroinflammatory markers mRNA expression inhibition by compounds 5d & 5f in brain hippocampal and cortex: A) Effect of compound 5d on TNF- α mRNA expression in the hippocampus; B) Effect of compound 5d on TNF- α mRNA expression in Cortex: C) Effect of compound 5d on IL-1 β mRNA expression in the hippocampus: D) Effect of compound 5d on IL-1 β mRNA expression in cortex: E) Effect of compound 5f on TNF- α mRNA expression in the hippocampus; F) Effect of compound 5f on TNF- α mRNA expression in Cortex: G) Effect of compound 5f on IL-1 β mRNA expression in the hippocampus: H) Effect of compound 5f on IL-1 β mRNA expression in the cortex. ***p < 0.001, **p < 0.01, *p < 0.05 vs scopolamine (SCP); #### p <	164

Fig. No.	Figure Legends	Page No.
	0.001 vs Naïve, NS = non-significant.	
5.44	Estimation of amelioration of $A\beta$ -induced of cognitive deficit effects of compound 5d and 5f through Morris water maze test; A) escape latency time (ELT) and B) the number of total platform crossings during the last 5 days of trials. Data represented as the mean \pm SEM (n=8).	165
5.45	Western blot analysis of protein expression in compound 5d and 5f treated mice hippocampus after ICV administration of $A\beta$; A) western blot representative bands, B) showing densitometric quantification APP/ $A\beta$; C) showing densitometric quantification BACE-1; D) showing densitometric quantification tau; E) showing densitometric quantification APP; F) showing densitometric quantification $A\beta$. Data represented as mean \pm SEM (n=3). ***p < 0.001, **p < 0.01, vs diseased.	166
5.46	Immunohistochemical analysis of BACE-1 and $A\beta$ expression levels in the hippocampal brain; A) showing immunohistochemical expression of BACE-1 and $A\beta$ expression effects in different animal groups; B) densitometric quantification of BACE-1 immunostains showing changes in % area (burden); C) densitometric quantification of $A\beta$ immunostains showing changes in % area (burden). ***p < 0.001 vs model (diseased) group, ns = nonsignificant. Data expressed as mean \pm SEM (n = 3).	167
5.47	(X) Histopathological estimation of the effects of compounds 5d and 5f on brain tissue via Nissl's staining after $A\beta$ -induced Morris water maze test A) Sham group hippocampus, CA1, CA3, and DG sections; B) $A\beta$ -induced group hippocampus, CA1, CA3, and DG sections; C) Donepezil (DNP) group hippocampus, CA1, CA3, and DG sections; D) Compound 5d treated group hippocampus, CA1, CA3 and DG sections; E) Compound 5f treated group hippocampus, CA1, CA3 and DG sections. (Y) The effect of compounds 5d and 5f in rescuing neuronal population in $A\beta$ -induced mice brain. The data is represented as mean \pm SEM (n=3). ***p < 0.001, vs Sham, ns = non-significant.	169

LIST OF SCHEMES

Scheme No.	Figure Legends	Page No.
1	Synthesis of targeted compounds (SD1-17)	56
2	Synthesis of the targeted Compounds (4a-j)	57
3	Synthesis of the targeted compounds (5a-q)	58

LIST OF TABLES

Table No.	Table caption	Page No.
1.1	Chemical structures, mechanism, and adverse effects of USFDA-approved drugs for the treatment of AD	13
5.1	<i>In vitro</i> ChE, and hBACE-1 inhibitory activity of the synthesized compounds	85
5.2	PI displacement assay and PAMPA-BBB permeability assay results of the compounds.	89
5.3	Liver and Kidney function tests of the experimental animals under acute toxicity studies	95
5.4	ADME predicted properties of the compounds and standard drugs	110
5.5	Results of docking (Glide score) and MM/GBSA.	111
5.6	The energy values of HOMO and LUMO orbital and energy gap of the identified hits.	124
5.7	Predicted ADME properties of the designed series of compounds.	126
5.8	Crystallographic data for compound 5f	142
5.9	IC ₅₀ values of the compounds (4a-j and 5a-5q) against hAChE, hBChE and BACE-1	145
5.10	Percentage PI displacement and PAMPA-BBB Permeability assay of selected compounds.	150

ABBREVIATIONS AND SYMBOLS

ACh	Acetylcholine
AChE	Acetylcholinesterase
AD	Alzheimer's disease
AFM	Atomic force microscopy
AMP	Adenosine monophosphate
AMPK	AMP-activated protein kinase
AP	Anterior – Posterior
ApoE	Apolipoprotein E
A β	Amyloid beta
APP	Amyloid precursor protein
ATCI	Acetylthiocholine iodide
ATR	Attenuated total reflectance
BACE-1	Beta amyloid cleaving enzyme 1
BBB	Blood-brain barrier
BChE	Butyrylcholinesterase
BSA	Bovine serum albumin
BTCI	Butyrylthiocholine iodide
CADD	Computer-aided drug design
CaMK	Ca ²⁺ /calmodulin dependent kinase
CAS	Catalytic anionic site
CAT	Choline acetyltransferase
CDCl ₃	Deuteriochloroform
CDK-5	Cyclin dependent kinase-5
ChE	Cholinesterase
CNS	Central nervous system
CoA	Coenzyme A
CoMFA	Comparative molecular field analysis
CoMSIA	Comparative molecular similarity indices analysis
COX	Cyclooxygenase
CREB	Cyclic-AMP-response element-binding protein
CST	Conjugated secondary antibody
CYP	Cytochrome P
DMSO	Dimethyl sulfoxide
DPP	Docking-post processing
DTNB	5,5-Dithio-bis-(2-nitrobenzoic acid)
DV	Dorsal - Ventral
Dyrk1A	Dual specificity tyrosine- phosphorylation-regulated kinase-1 A
EDGs	Electron donating groups
EDTA	Ethylenediaminetetraacetic acid
ELT	Escape latency time
ERK	Extracellular signal-regulated protein kinases

EtOH	Ethanol
EWGs	Electron withdrawing groups
FDA	Food and drug administration
FRET	Fluorescence resonance energy transfer
FT-IR	Fourier-transform infrared spectroscopy
GSK-3 β	Glycogen synthase kinase-3 β
hAChE	Human AChE
hBChE	Human BChE
HPLC	High performance liquid chromatography
HTVS	High throughput virtual screening
i.p.	Intraperitoneal
ICV	Intracerebroventricular
JNK	Janus kinase
LBDD	Ligand-based drug design
MAO-B	Monoamine oxidase-B
MAPK	Mitogen activated protein kinase
MARK	Microtubule affinity-regulating kinase
MDA	Malondialdehyde
ML	Medial – Lateral
MM-GBSA	Molecular mechanics generalized Born surface area
mp	Melting point
MTT	3-(4,5-Dimethylthiazol-2-yl)-2,5-diphenyl-tetrazolium bromide
Na-CMC	Sodium carboxymethyl cellulose
NADPH	Reduce form of nicotinamide adenine dinucleotide phosphate
NFI	Normalized fluorescence intensity
NFTs	Neurofibrillary tangles
NMDAR	<i>N</i> -Methyl-D-aspartate receptor
NMR	Nuclear magnetic resonance spectroscopy
NOS	Nitric oxide synthase
NO _x	NADPH oxidase
NPT	Normality, pressure and temperature
OECD	Organisation for economic co-operation and development
OPLS	Optimized potential for liquid simulations
p.o.	Per oral
PAMPA	Parallel artificial membrane permeation assay
PAS	Peripheral anionic site
PBL	Porcine brain lipid
PBS	Phosphate buffered saline
PBST	Phosphate buffered saline with Tween 20
PDB	Protein data bank
PDE	Phosphodiesterase
PHFs	Paired helical fibrils

PI	Propidium iodide
PKA	Protein kinase-A
PPs	Protein phosphatases
PTPA	Protein tyrosine phosphatase-A
QSAR	Quantitative structure-activity relationship
RIPA	Radioimmunoprecipitation assay
RMSD	Root mean square deviation
RNS	Reactive nitrogen species
ROS	Reactive oxygen species
SBDD	Structure-based drug design
SFKs	Src family non-receptor tyrosine kinases
SOD	Superoxide dismutase
SP	Standard precision
TBARS	Thiobarbituric acid reactive substances
TBST	Tris-buffered saline with Tween 20
TLC	Thin layer chromatography
TPKI	Tau protein kinase-I
TRITC	Tetramethylrhodamine isothiocyanate
UV	Ultraviolet spectroscopy
VSGB	Variable surface generalized Born
WHO	World Health Organization
XO	Xanthine oxidase
XP	Extra precision
XRD	X-ray diffraction

SYMBOLS & UNITS

$\times g$	Relative centrifugal force
$^{\circ}\text{C}$	Degree Celsius
μL	Microliter
μm	Micrometer
μM	Micromolar
\AA	Angstrom
α	Alpha
β	Beta
γ	Gamma
ν	Wavenumber
cm	Centimeter
d	Doublet
dd	Doublet of doublets
ddd	Doublet of doublets of doublets
equiv	Equivalent
g	Gram

h	Hour
Hz	Hertz
<i>J</i> -value	Spin-spin coupling constant
K	Kelvin
kg	Kilogram
KHz	Kilohertz
m	Multiplet
mg	Milligram
min	Minute
mL	Milliliter
mM	Millimolar
ng	Nanogram
nm	Nanometer
q	Quartet
RH	Relative humidity
rpm	Rotations per minute
s	Seconds/Singlet
t	Triplet
td	Triplet of doublets
U/mL	Units per milliliter
v/v	Volume by volume
w/v	Weight by volume

PREFACE

Alzheimer's disease (AD) is considered to be an enormous healthcare problem caused by the loss of neurons and synapses, particularly in the neocortex and hippocampus. AD results in remarkable structural and functional damage to the brain, which resulted in severe behavioral alterations and cognitive dysfunction. A recent report 2018 from World Health Organization (WHO) accounts for 50 million cases of AD worldwide and this figure is estimated to be tripled by 2050. There are several underlying pathophysiology associated with the progression of cognitive deficits in AD condition that includes, lower acetylcholine (ACh) levels in the synaptic cleft, amyloid beta ($A\beta$) aggregation and deposition, *N*-methyl-D-aspartate receptor (NMDAR) activation, oxidative stress in response to neuroinflammation, tau hyperphosphorylation that results in generation of neurofibrillary tangles (NFTs), genetic mutation in apolipoprotein E4 ($APO\epsilon 4$), etc.

The current treatment strategy for AD involves the use of some FDA-approved drugs which only provide symptomatic relief to the patient. Certain FDA-approved medications such as AChE inhibitors (donepezil, rivastigmine, and galantamine) and NMDA receptor antagonists (memantine) are being used for the treatment of AD. Recently, Aducanumab and Lecanemab (monoclonal antibodies) have been approved by FDA in an accelerated approval pathway as a disease-modifying therapy for AD, though their use is still controversial in AD progression.

This research work in this thesis was divided into two parts; the first part of the thesis describes the design, synthesis, and biological evaluation of a novel series-I (**SD1-17**) compounds against hAChE, hBChE, hBACE-1, and $A\beta$ aggregation inhibitory potentials. A detailed *in vivo* study of the most active compound of the series was also performed in scopolamine and $A\beta$ -induced behavioral rat models of AD following *ex-vivo* biochemical estimation, and histopathological examination of brain tissue slices to

observe any neuronal tissue damage. The *in silico* molecular docking and Molecular dynamic simulation studies were also performed to confirm the ligand-protein complex's stability.

The second part of the thesis demonstrates the successful design and synthesis of a new class of compounds using *in silico* e-Pharmacophore hypothesis. A novel series II & III were designed as multitarget-directed ligands to discover new agents for Alzheimer's disease treatment. All the compounds were tested for their *in vitro* inhibitory potential against hAChE, hBChE, hBACE-1, and A β aggregation. The neurotoxic liabilities of the compounds were also tested against RA/BDNF differentiated SH-SY5Y neuroblastoma cell lines. Both the scopolamine and A β -induced mouse models for AD were studied to evaluate the learning and memory behavior improvements after treatment with the most active compounds of the series. *Ex vivo* studies of hippocampal and cortex brain homogenates were performed to investigate the oxidative stress biomarker and pro-inflammatory cytokines (TNF- α , and IL-6 mRNA) levels. The histopathological examination was performed to observe neuronal appearance in the hippocampal and cortex region of the brain. Western blot analysis and immunohistochemical analysis were also performed to investigate the A β , APP/A β , BACE-1, and tau protein molecular expression levels.

The work has been presented in this dissertation under the following sections:

Chapter 1: This chapter flashes the light on AD, its development & progression, etiology, and various pathophysiology associated with AD. This chapter also deals with the current treatment strategy for AD, a newer designing approach to tackle the disease progression that includes mainly molecular hybridization, and computational methods.

Chapter 2: This chapter describes a detailed literature survey on benzylpiperidines and 1,3,4-oxadiazoles, piperazine, and N-benzylpiperidine derivatives as multitarget directed ligands (AChE, BChE, BACE-1, and A β).

Chapter 3: This chapter summarizes the research objectives of the overall study, the rationale for performing different *in vitro* and *in vivo* investigations, and a detailed plan of work that is exemplified in this thesis.

Chapter 4: This chapter describes the experimental procedure used in the synthesis, characterization, protocols for computational studies, and *in vitro* and *in vivo* pharmacological evaluations.

Chapter 5: This chapter covers the overall findings as results and discussion part of the research work.

Chapter 6: Describes the summary and conclusion of the presented work.

Chapter 7: This section includes the references as a source of information to carry out the research work.

Chapter 8: An appendix consisting of the NMR (^1H and ^{13}C) and Mass spectra along with HPLC chromatograms of the representative compounds followed by a list of published papers and presentations at international conferences.